Complex dielectric function of amorphous diamond films deposited by pulsed-excimer-laser ablation of graphite

Fulin Xiong, Y. Y. Wang, and R. P. H. Chang
Department of Materials Science and Engineering and Materials Research Center, Northwestern University, 2225 North Campus Drive, Evanston, Illinois 60208
(Received 8 April 1993)

Amorphous diamond films have been synthesized by pulsed excimer- (ArF) -laser ablation of graphite at room temperature. Detailed studies of the energy-dependent complex dielectric function in the energy range up to 40 eV have been carried out by Kramers-Kronig dispersion analysis of transmission electron-energy-loss spectroscopy and spectroscopic ellipsometry. Distinct from those of graphitic amorphous carbon and diamondlike carbon, the optical constants of amorphous diamond films are closely related to those of crystalline diamond, but with a smooth structure, a decrease in strength, and band shift towards lower energies. The variation of the dielectric function from crystalline diamond to amorphous diamond is analogous to that of crystalline and amorphous semiconductors such as Si and Ge. The extracted optical energy band gap reaches 2.6 eV, the highest value among the reported results for amorphous carbon films. The study of the dielectric function and its relation to the band structure of amorphous diamond films has also confirmed their diamond character. All of this information provides further evidence of the existence of amorphous diamond.

I. INTRODUCTION

Diamond and graphite are two basic allotropic crystalline structural forms of elemental carbon,[1] though a variety of cluster forms (fullerenes) have been discovered recently. In diamond, carbon atoms are connected in a fourfold-coordinated tetrahedral bonding structure (sp^3 hybrids, four σ bonds per carbon atom); while in graphite, the atoms are in a threefold-coordinated hexagonal bonding planar structure (sp^2 hybrids, three σ bonds plus one π bond per carbon atom). These two bonding structures result in distinct properties in all aspects for the two crystalline carbon forms. Graphite is thermodynamically stable with respect to diamond at standard temperature and pressure (for the transition from diamond to graphite, $\Delta H = -2.1$ kJ/mol).[1] As a consequence, amorphous carbon (a-C), a common carbon form, is mostly a disordered graphitic network. Both theoretical study and experimental evidence have shown that over 80% of the carbon atoms in thermally evaporated a-C films are sp^2 bonded.[2,3] An amorphous form of diamond or a completely tetrahedrally bonded amorphous carbon network was previously thought to be unlikely to exist because of the presumed bonding constraints imposed on a carbon network,[4,5] even though such a tetrahedral amorphous structure is common in other column IV elemental semiconductors, such as Si and Ge.

During the course of synthesis of polycrystalline diamond by low-temperature and low-pressure chemical-vapor deposition processes, amorphous diamondlike carbon (DLC) has attracted renewed attention[4,6] because this material has been found to have physical, chemical, and mechanical properties similar to those of crystalline diamond. Early attempts to make diamondlike carbon films include the introduction of hydrogen atoms (20–60 %) to saturate the dangling bonds of carbon atoms, so that the sp^3 character in the films is due to C-H bonds instead of to C-C bonds. Although the hydrogenated amorphous carbon films have a large optical energy band gap (1–2 eV) and high mechanical hardness, heating of the films causes hydrogen to escape, resulting in soft graphitic carbon films.[7,8]

Recently, a variety of techniques such as pulsed-laser deposition,[9–13] filtered arc deposition,[14,15] and ion beam deposition[16,17] have been used for the deposition of diamondlike carbon films without incorporated hydrogen. Such films with a high degree of diamond character are referred to as amorphous diamond (a-D).[18,19] It was suspected that in this material, though lacking the long-range order of a crystalline structure, the local bonding structure remains closer to sp^3 rather than sp^2. This has been revealed in the neutron diffraction and electron-energy-loss spectroscopy analysis.[18,19] However, Raman spectroscopy measurement of this material does not show the distinct feature appearing in crystalline diamond. Due to these conflicting experimental findings, it is still arguable whether this newly developed material is amorphous diamond with its local bonding structure in an sp^3 form.

We have deposited amorphous diamond films by pulsed ArF-excimer-laser ablation of graphite at room temperature.[13] In this paper we present a detailed study of the energy-dependent complex dielectric function of a-D films in the energy range up to 40 eV. The dielectric function provides not only the corresponding optical constants of the material, but also gives additional information about the electronic band structure of the material. The dielectric function of the films is determined by a Kramers-Kronig (KK) dispersion analysis of transmission high electron-energy-loss spectroscopy (EELS) and

0163-1829/93/48(11)/8016(8)/$06.00

spectroscopic ellipsometry (SE). The results are compared with the dielectric function of crystalline diamond. Analogous to the relationship between dielectric functions of amorphous and crystalline silicon and germanium, we show further evidence of the existence of amorphous diamond and the sp^3 local structure in the films.

II. EXPERIMENTAL

The *a-D* films in this study were deposited by pulsed ArF- (193 nm wavelength) excimer-laser ablation of pyrolytic graphite (PG) at room temperature in a high-vacuum chamber. The detailed description of the deposition system and process conditions was presented elsewhere.[13,20] Si(100) substrates were cleaned through a standard decreasing process and finally dipped in diluted HF acid to remove the native SiO_2 before loading into the chamber. The as-deposited films on Si wafers were mirrorlike smooth. After removing the substrates, the free-standing films were transparent. General properties of *a-D* films have been characterized by a variety of analytic techniques,[13] which we summarize briefly here. The plan-view transmission electron microscopy and selected area electron diffraction indicated that the films were homogeneous and in an amorphous phase. The films were tested to be chemically inert, electrically resistant, and optically transparent in the IR and visible regions. High-energy ion elastic forward scattering spectroscopy revealed that the films were free of hydrogen, a distinct difference from diamondlike hydrocarbon films. Nanoindentation measurements showed a microhardness close to 40 GPa (80–100 GPa for crystalline diamond) and a Young's modulus value of about 220–230 GPa. The optical energy gap was found to be 2.6 eV, the highest value reported for any *a-D* or DLC films prepared previously by pulsed-laser deposition or filtered cathode arc deposition. The *a-D* films also exhibited excellent thermal stability, and the optical energy band gap remained unchanged upon annealing up to 800 °C in vacuum. This is in contrast to the hydrogenated diamondlike carbon films which upon heating turn to soot. Films deposited on Si(100) with a thickness of about 150 nm were used for ellipsometry measurements, and films deposited on Si or freshly cleaved NaCl crystalline substrates with a thickness of 30–50 nm were used for EELS analysis. The specimens were made by lifting the film onto a Cu grid after removing the Si substrates by chemical etching or dissolving the NaCl in water.

Spectroscopic ellipsometry measurements were performed on a rotating analyzing ellipsometry system (SOPRA, Inc.) for the films deposited on Si(100). Spectropscopic scanning covered a range from 1.5 to 5 eV. A microspot of a size of 150×100 μm^2 was used to eliminate the effect of thickness nonuniformity of the films. An incident angle of 75° with respect to the sample surface normal was used. The optical properties of the films, i.e., the real and imaginary parts of the complex refractive index ($N=n+ik$), were obtained by polynomial fitting of the experimental curves in a three-layer (air-film-substrate) structure with the Cauchy model,[21]

$$\begin{aligned} n &= A_1 + A_2/\lambda^2 + A_3/\lambda^4 , \\ k &= B_1 + B_2/\lambda + B_3/\lambda^3 , \end{aligned} \tag{1}$$

where λ is the photon wavelength, and A_i and B_i are the coefficients determined by the least-squares fit to the spectroscopic ellipsometry spectra. The complex dielectric function ($\varepsilon=\varepsilon_1+i\varepsilon_2$) was derived through the relation

$$\varepsilon = N^2 = (n+ik)^2 = (n^2-k^2)+i2nk . \tag{2}$$

Based on the dielectric theory,[22] the electron-energy-loss spectrum can be quantitatively described by

$$\frac{dI(\Delta\omega,\Delta\Omega)}{d\omega d\Omega} \propto \mathrm{Im}[-1/\varepsilon(\omega)] = \varepsilon_2/(\varepsilon_1^2+\varepsilon_2^2) . \tag{3}$$

The dielectric function of an isotropic solid can be readily determined from an EELS spectrum[23,24] through the KK dispersion analysis:

$$\mathrm{Re}[1/\varepsilon(\omega)] = 1-(2/\pi)\int_0^\infty [\xi/(\xi^2-\omega^2)] \times \mathrm{Im}[-1/\varepsilon(\xi)]d\xi . \tag{4}$$

At $\omega=0$, Eq. (4) gives a normalization condition for the energy-loss spectra providing ε_0 is known. EELS measurements were carried out on a Hitachi H-2000 analytical transmission electron microscopic, operated at an accelerating voltage of 100 keV. The microscope was equipped with a cold field-emission gun with an energy spread of about 0.5 eV [full width at half maximum (FWHM)], and with a Gatan-666 parallel electron-energy-loss spectrometer. Two regions of EELS spectra were collected, the low-energy valence excitation loss spectra (0–80 eV) and the high-energy carbon *K*-edge core-loss spectra (250–400 eV). The low loss spectrum was taken at an off-angle scattering angle with a momentum transfer of 0.1 A^{-1} in order to avoid complications with the contributions from surface plasmons, Čerenkov radiation, and energy-dependent factors. The energy-loss function was obtained from the low loss spectra by the zero loss peak removal with a Lorentzian function fitting, and the multiple scattering correction up to the third order.[25] In the calculation, the loss function was extended to infinite energy as $1/E^3$ for $E>80$ eV.[23,24] The dielectric function was calculated from the electron-loss function by KK analysis in conjunction with the spectroscopic ellipsometry result for the normalization constant, ε_0.

III. RESULTS

The experimental spectroscopic ellipsometry spectra ($\tan\Psi$, $\cos\Delta$) of a film deposited on Si(100) are given in Fig. 1. From the spectra, the oscillation strength of $\cos(\Delta)$ between -1 and $+1$ indicates that the film is smooth on the surface and optically transparent. The best-fit spectra from the Cauchy polynomial approximation are also plotted as the solid line in Fig. 1. The derived refractive index spectra for this film are shown in Fig. 2. The n spectra for diamond[26] and graphite[27] are also plotted in the same figure for comparison. The real part of the index of refraction (n) had a trend similar to

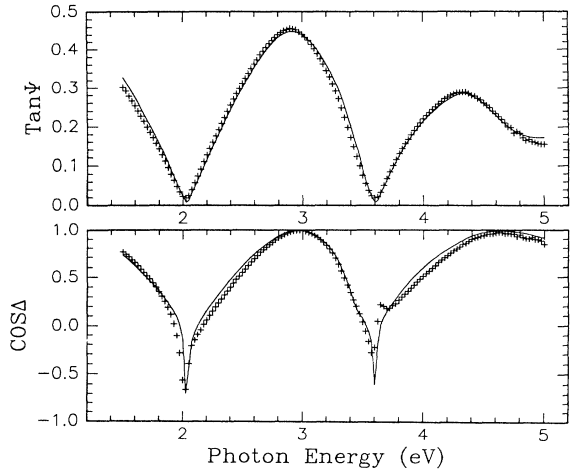

FIG. 1. Spectroscopic ellipsometry spectra of amorphous diamond on Si(100) prepared by pulsed-excimer-laser ablation. Solid curves are the best fits of a polynomial function using the Cauchy model.

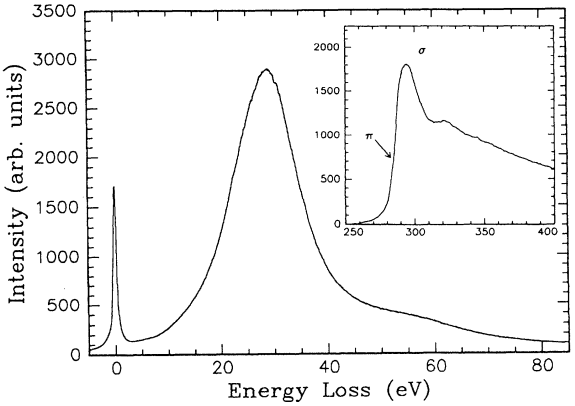

FIG. 3. Low-energy-loss spectrum of electron-energy-loss spectroscopy of an *a-D* film on Si(100). Insert: The corresponding carbon *K*-edge core-loss spectrum after removing the background.

that of diamond, but different from that of graphite. Its values range between 2.5 and 2.8, slightly higher than diamond. The k value is very low in this region with a cutoff at 1.8 eV, implying a high optical energy band gap. A linear extension of the n spectrum to zero energy gives $n_0=2.45$, resulting in $\varepsilon_0=6.0$, slightly higher than that of crystalline diamond (*c-D*).

Figure 3 shows a low loss EELS spectrum of an *a-D* film. The spectrum gives features distinctly different from that of graphite, consisting of only a single broad plasmon peak centered at 29.5 eV (compared to 26 eV for graphite and 33 eV for *c-D*). The peak at 60 eV is the second-order plasmon loss. The π-π^* antibond transition peak (presented at about 6–7 eV in the spectra of graphite and evaporated *a-C* films) is completely absent, indicating little or no sp^2 bonding in the film. The insert in Fig. 3 is the corresponding carbon *K*-edge loss spectrum after removal of the background. The spectrum of our film gives a broad peak centered at 296 eV, a smearing out of the fine transition structures from 1*s* to σ^* states, with the overall structure close to that of diamond.[13] A very small shoulder at the low-energy edge of the carbon *K*-edge loss band indicates the existence of a small fraction of π bandlike transition in the film. The estimated sp^3 bond fraction in the film is greater than 95%.

The energy-loss function of *a-D* deduced from the EELS low loss spectra is shown in Fig. 4. The low-energy region has been modified according to the loss function spectrum calculated from the ellipsometry result. The dashed line refers to the case before multiple scattering is made. The resulting real and imaginary parts of dielectric function of *a-D* by the KK analysis are given in Fig. 5. The dielectric function from spectroscopic ellipsometry measurements in the energy range of 1.5–5 eV is also plotted. Two results are consistent in the energy range that the ellipsometry covers. For comparison, the plots of the energy-dependent complex dielectric function of crystalline diamond from Ref. 26 are also given in Fig. 5. In addition, the spectra of the dielectric function of crystalline and amorphous silicon[28,29] are also inserted in Fig. 5.

The main feature in the spectra of *a-D* shows smooth single bands with an overall structure close to *c-D*, but

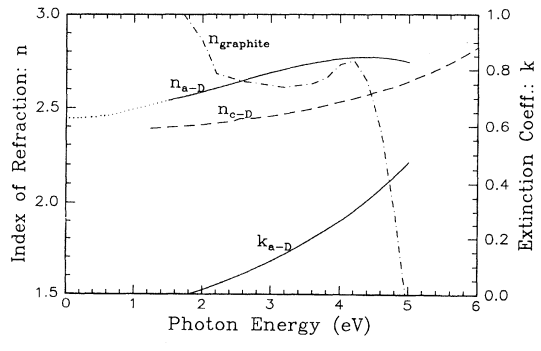

FIG. 2. Real part (n) and imaginary part (k) of the complex refractive index of an *a-D* film, reduced from the spectroscopic ellipsometry measurement shown in Fig. 1. The n values for diamond (from Ref. 26) and graphite (from Ref. 27) are also plotted for comparison.

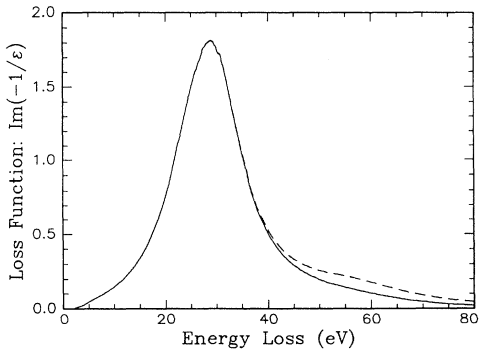

FIG. 4. Energy-loss function of amorphous diamond, reduced from EELS spectrum shown in Fig. 3. Dashed curve is before multiple scattering correction.

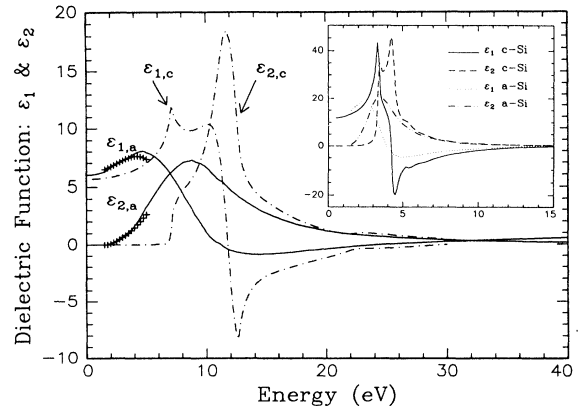

FIG. 5. Complex dielectric function of amorphous diamond reduced from the energy-loss function shown in Fig. 4 through K-K analysis (solid curves, $\varepsilon_{1,a}$ and $\varepsilon_{2,a}$). Crosses are the results from SE shown in Fig. 2. Complex dielectric functions of crystalline diamond from Ref. 26 are also plotted as dot-dashed curves. Insert: Plots of the complex dielectric function of crystalline and amorphous silicon for comparison.

distinct from that of graphite.[30] The position of the peaks shift to lower energies, with a peak broadening and a magnitude drop. The $\varepsilon_{1,\max}$ of 8 occurs at 4.5 eV, which is 1.5 eV lower than the energy position in c-D. This has been revealed in the SE result. In ε_2 the absorption band is peaked at 9 eV, shifted by about 3 eV from the maximum position in c-D. The magnitude of the band drops to 7.2 with a width of 8 eV in FWHM, compared to a peak value of 18.5 and a width of 2.5 eV in FWHM for c-D. In the energy region higher than 20 eV, both ε_1 and ε_2 values closely approach those of c-D. The overall view of the dielectric function explains why the refractive index in the visible region measured by ellipsometry is always higher than that of c-D.

IV. DISCUSSION

The overall features of the dielectric function of the a-D films we obtained possess characteristics common to those of amorphous semiconductors. Such a spectroscopic variation of dielectric function from the crystalline to the amorphous state is present clearly in Si (Fig. 5) and Ge.[31] The a-D, a-Si, and a-Ge all share smoothly varying spectra, a decrease in magnitude, and a bandshift toward lower energies in their dielectric functions. It is generally agreed that the variation of the dielectric function from crystalline to amorphous materials is attributed to the loss of long-range order in the amorphous state which leads to the relaxation of the k-conservation selection rule, resulting in the smoothing out of the fine band structure in dielectric function spectra.

We consider the optical transition strength $\omega^2\varepsilon_2(\omega)$ which is related to the density of states of the valence and conduction bands, $g_c(E)$ and $g_v(E-E_g)$,[32,33] as

$$\omega^2\varepsilon_2(\omega)=\text{const}\int_0^{\hbar\omega} g_c(E)g_v(E-E_g)dE \ . \tag{5}$$

In an amorphous semiconductor, the conduction-band density of states $g_c(E)$ should be smooth and featureless and can be reasonably taken as a step function at an energy above the valence-band mobility edge.[34] Thus, from Eq. (5), the optical transition strength $\omega^2\varepsilon_2(\omega)$ is proportional to the integral of the density of valence-band states, implying the dependence of the absorption band (or ε_2) on the density of the valence states. Though this correlation cannot give an exact representation of the valence-band density of states, it exhibits their major features. The plots of the quality of the optical transition strength $\omega^2\varepsilon_2(\omega)$ in terms of the transition energy for a-D and c-D are shown in Fig. 6. The remarkable structural differences between them are obvious. These indicate a reduction and difference in the distribution of the density of valence-band states and weakening in the valence electron bonding strength in a-D. We have also noticed the absorption mobility edge shift toward the low-energy edge with a broad diffuse tail. This is directly attributed to its amorphous structure. The presence of a great number of voids and dangling bonds as well as changes in bonding in the first- and second-nearest-neighbor region may result in such a shift and magnitude drop. The broad tail in the low-energy region suggests that there may exist defect-related states in the valence-band tail, possibly extending into the band gap. Theoretical considerations of such sp^2-free a-D carbon networks by Robertson and O'Reilly[35] in a calculation of the local density of states of electrons by the recursion method revealed a smoothing of features and a shift of the leading edge of the valence band. The results are consistent with our perception of the transition strength obtained from the dielectric function of a-D.

As an implication of the connection of the band structure with the dielectric function, the optical energy band gap can be determined from the relation[33,36]

$$\omega^2\varepsilon_2(\omega)=\text{const}(E-E_g)^2 \ , \tag{6}$$

assuming the band edges are parabolic. We have determined the optical energy band gap to be 2.6 eV for our a-D films from spectroscopic ellipsometry results.[13] In Fig. 7, we extend this plot to a higher-energy region from the ε_2 spectrum of a-D. There, the extrapolation by a straight line along the edge indicates the satisfaction of the square power law. This result is an indication of the

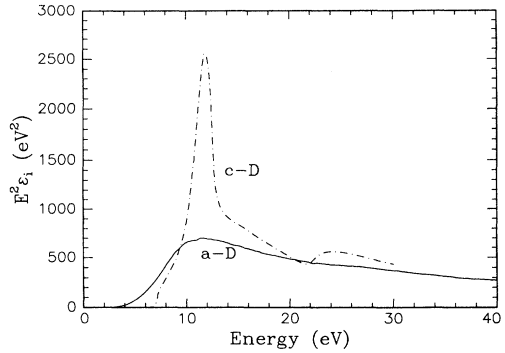

FIG. 6. The energy-dependent optical transition strength of amorphous diamond and crystalline diamond.

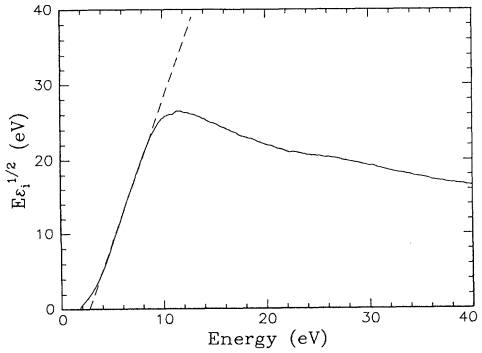

FIG. 7. Plot of the quantity $E\varepsilon_i^{1/2}$ vs the photon energy, E, from the data shown in Fig. 6 for an amorphous diamond film.

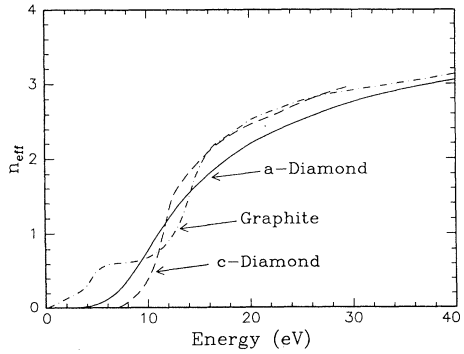

FIG. 8. The energy-dependent oscillator strength or the effective number of valence electrons per atom contributing to interband transitions in amorphous diamond, crystalline diamond, and graphite.

consistency between EELS and ellipsometry measurements.

The similar character of tetrahedral bonding in a-D to c-D can also be recognized by examining the oscillator strength, n_{eff}, the effective number of valence electrons per carbon atom which take part in optical transitions[37,38] up to an energy E_0,

$$n_{\text{eff}}=(m/2\pi^2Ne^2\hbar^2)\int_0^{E_0}E\varepsilon_2(E)dE\ , \tag{7}$$

where N is the atomic density of the material. For the column IV elemental atoms such as silicon and carbon, there are four valence electrons per atom available for bonding. If they were all to take part in interband optical transitions, we would expect n_{eff} to take a value of 4 at sufficiently high energy, providing that all the possible optical transitions are exhausted and the transitions involving the core states are negligible. Both crystalline and amorphous silicon closely follow this tendency.[39] In the materials of carbon, however, the behavior is different between diamond and graphite. In diamond, four sp^3-bonded σ electrons are available for valence-to-conduction-band transitions. Thus, n_{eff} would rise sharply after passing through a band-gap threshold and approach a value of 4 at a sufficiently large energy. This is shown in Fig. 8. It is calculated from the dielectric function shown in Fig. 5 from Ref. 26. Below 7 eV, n_{eff} is zero, indicating a wide band gap for c-D. There is a rapid increase at 10 eV, and n_{eff} reaches 3 at 30 eV. It tends to approach 4 at higher energies. In contrast, for graphite, because of its sp^2 bond, the π-π^* transitions result in a plateau in n_{eff} at 0.6 electrons below 9 eV. This spectrum is illustrated in Fig. 8, which is calculated from the data given in Ref. 27. Although there is one π electron and three σ electrons involved in the transition, the fact that the number of electrons below 9 eV is about 0.6 indicates that the π-π^* transition has not saturated at 9 eV. From our experimental results given in Fig. 6, the n_{eff} for a-D as a function of the energy is calculated and shown as the solid curve in Fig. 8. The behavior of n_{eff} for a-D is very similar to that of diamond and clearly different from that of graphitic carbon since there is no evidence of the existence of a plateau at low energies. In a-D, $n_{\text{eff}}=0$ for energies below the absorption edge. It rises less rapidly and reaches a value of 3.5 at the energy of 40 eV. It is also expected to reach a value of 4 at sufficiently high energies.

We note that an error, a missing factor of $\pi/2$, has been found[3,26,40] in the report of Taft and Phillipp,[30] where it was shown that the π-π^* electron oscillator strength in graphite saturated at 9 eV with 1 electron/atom, instead of 0.6 electron/atom. Taft and Phillipp's result was widely quoted by later publications with an implication for the quantitative determination of the relative fraction of sp^2 and sp^3 bonds from the behavior of the complex dielectric function below 9 eV.[8,33] However, because the π electron transition does not saturate above 9 eV, contrary to what was believed earlier, it is clear that the relative fraction of sp^2 and sp^3 bonds cannot be simply determined from the behavior of the oscillator strength below 9 eV. This view is also supported by theoretic calculations of the distribution of density of states for graphite by Robertson and O'Reilly,[35] which indicates that the transition for π electrons can be extended in the energy region greater than 9 eV.

From the electron-energy-loss function and dielectric function, the density of the film can be estimated from the plasmon energy in the "free-electron gas" model for the valence electrons[22] as

$$\omega_P^2=\bar{\omega}_P^2-\omega_n^2=4\pi Ne^2/m\ . \tag{8}$$

where $\bar{\omega}_P^2$ is the valence plasmon energy observed in EELS and ω_n is the center of valence-band excitation in the dielectric function ε_2. Assuming that 4 electrons per carbon atom participate in the plasma transition, we estimate the density of our films to be 2.95 g/cm^3, providing the valence plasmon energy at 30 eV and the center of excitation at 9 eV. This density is about 18% lower than that of crystalline diamond (3.515 g/cm^3), but 30% higher than that of graphite (2.26 g/cm^3). A similar value has been found for the films deposited by other methods such as filtered arc deposition,[18,41] pulsed-laser deposition,[12] and ion beam deposition.[17] Reduction of the mass density from that of its crystalline form can be found in most solids. It is mainly due to the reduction of

its atomic coordination number in the amorphous random network and the existence of a large fraction of voids.

The dielectric function of our films as well as its implication for band-structure analysis have provided further evidence for the confirmation of the reality of *a-D* films. With its hydrogen-free character, fulfilled sp^3 bonding structure, unique physical, chemical, and mechanical properties, and analogous transition changes of dielectric function and optical properties from its *c-D* counterpart as parallel by those of *a*-Si and *c*-Si, the designation of amorphous diamond is completely satisfied. However, we have noticed that the detailed properties of this material can be varied, depending strongly on the preparation conditions, especially the energetic sources used for deposition. As the energy of the depositing carbon species spans the range from thermal to high energy (a few tens of eV), the films can span the range from the completely graphitic *a*-C, diamondlike, to *a-D*. In our case, the ArF excimer laser we used with a short UV wavelength (193 nm, 6.2 eV) and a short pulse width provides a high efficiency of ionization and excitation for atomic carbon deposited species with a high kinetic energy (up to 50 eV). These ensure the properties of the deposited films to be near those of diamond.

The properties of *a-D* and diamondlike *a*-C films have been extensively studied and characterized in many aspects. The main effort was on the determination of physical properties, mechanical hardness, and the bonding structure. Among the variety of techniques used for deposition of carbon films with a tendency towards *a-D* films, pulsed-excimer-laser deposition[12,13] and filtered arc deposition[14,15] have shown great promise. Plasma arc deposited hard carbon films (referred to as *a-D*) have been extensively studied by Saeed and co-workers.[18,19,41–43] They show that amorphous films have structures essentially analogous to the other elemental amorphous semiconductors (Si and Ge). Tetrahedral bonding up to 85% has been found with the rest trigonal bonding. The films have been also found to contain up to 11% hydrogen. The residual sp^2 π bonding has been shown significantly in the EELS spectra. Hard hydrocarbon films from a gas plasma deposition have been studied by Fink *et al.* with EELS.[8]. Though the film had an optical energy band gap of 2.05 eV, the appearance of sp^2 bands in the EELS spectra and degrading of diamondlike properties upon annealing exclude them from the *a-D* category. Ion-beam-sputtering-deposited films by Cuomo *et al.*[17] have shown a strong dependence of the sp^3/sp^2 ratio and mass density on deposition conditions, while a graphitic character has been shown in the ion-beam-sputtering-deposited films by Savvides.[33] The films deposited by pulsed-excimer-laser ablation with KrF (248 nm) beam by Pappas *et al.*[12] had an sp^3 bond fraction up to 75% on nondiamond substrates with the optical energy band gap up to 1.8 eV. In comparison, our films prepared by pulsed-excimer-laser deposition with an ArF beam give superior quality with the highest optical energy band gap (2.6 eV) obtained so far.

Common critical features for the formation of *a-D* are believed to rely on nonequilibrium features in the deposition process,[44] in which the carbon species impact the substrate at energies well above thermal energies and quickly quench down to the comparatively lower substrate temperatures, referred to as an energy condensation process. We suggest that for the formation and structural phase stability of this *a-D* material, the initial atomic ionization and excitation of deposited carbon species and their kinetic energy range are very important factors, which provide the precondition for a bonding transition from the planar sp^2 to three-dimensional sp^3. After these carbon species are accommodated on the substrate surface through the energy condensation process, the compressive stress in the film generated would further stabilize the sp^3 bonding structure. This effective pressure and temperature condition in the film could match a condition falling inside the diamond stable zone as is proposed by McKenzie *et al.*[18,19]

By reviewing the reported results on *a*-C films prepared by laser ablation methods, we have found[45] that there is a strong correlation between the wavelength of lasers used for ablation and the optical energy band gap of the resulting films. As the laser wavelength changes from the IR region (the photon energy of $\sim$1 eV) to UV region ($\sim$5–6 eV), the optical energy band gap of the films increases consistently from 0 up to 2.6 eV. We suspect that upon the laser impact on a graphite target, the original sp^2 C-C bonding in the target material would be destroyed due to laser-induced high-temperature rapid heating, ionization, and excitation. A plasma plume with highly ionized and highly energetic carbon species is generated. Depending on the laser photon energy used, carbon species in the plume can be at different excitation states, ejecting in cluster forms with a kinetic energy of a few eV for IR laser sources to a mostly atomic ionized form with a kinetic energy of a few tens eV for UV excimer lasers.[46–48] Based on this precondition, these highly ionized or excited carbon species have a tendency in a different degree to reconstruct themselves into sp^3 C-C bonding. Thus, in the deposited films prepared by different laser sources, instead of a simple mixing of standard sp^2 and sp^3 bonds, there may exist an evolutional transition in the bonding structure formation from the planar sp^2 to three-dimensional sp^3 with respect to changes of the bond angle and length or bond interaction strength. In turn, this evolution leads to film property changes from graphitic to diamondlike. The supporting experimental evidence has been illustrated in plasma arc deposited amorphous carbon films by Mckenzie *et al.*[18] As the plasma energy spans from 22 to 33 eV, the nearest C-C distance, measured by neutron scattering, changes from 0.142 nm (for graphite) to 0.154 nm (for diamond). In the $(e,2e)$ analysis,[3] it is also demonstrated that there is a rehybridization between π and σ electrons in ion beam deposited DLC films due to the bending of the planar σ bonds. More theoretical and experimental studies are needed to confirm such behavior in the case of pulsed-excimer-laser deposition of *a-D* films.

V. CONCLUSIONS

Amorphous diamond has been synthesized by pulsed-excimer-laser deposition. Its measured dielectric func-

tion has provided further evidence to confirm its existence. The dielectric function of *a-D* presents a typical characteristic of tetrahedrally bonded semiconductors. Loss of a long-range periodic crystalline structure in *a-D* leads to a smooth band feature. Its overall behavior contrasts sharply to graphite but is similar to that of crystalline diamond. The peak position in the dielectric function shifts to a low-energy region, with a magnitude drop and bandwidth broadening, leading to a narrow optical band gap and an absorption tail at low energies. The measured optical energy band gap of our films is 2.6 eV, the highest value reported so far for pulsed-laser deposited amorphous carbon films. The variation of the dielectric function from crystalline to amorphous diamond is analogous to the variation seen for crystalline to amorphous semiconductors such as Si and Ge. Implications of the dielectric function of *a-D* further show that the transition strength and oscillator strength of *a-D* are very much in connection with those of *c-D*. The films we obtained have shown a high degree of diamond character upon the retaining of the sp^3 bonding in a short-range order.

ACKNOWLEDGMENTS

This work was supported in part by the Department of Energy (Contract No. DE-FG02-87ER45314) and the Office of Naval Research. The research made use of Materials Research Laboratory Central Facilities supported by a National Science Foundation grant to Materials Research Center of Northwestern University (DMR-91-20521).

[1]H. Marsh, *Introduction to Carbon Science* (Butterworths, London, 1989).
[2]J. Robertson, Adv. Phys. **35**, 317 (1986).
[3]G. Gao, Y. Y. Wang, A. L. Ritter, and J. R. Dennison, Phys. Rev. Lett. **62**, 945 (1989).
[4]J. C. Angus and C. C. Hayman, Science **241**, 913 (1988).
[5]J. C Angus and F. Jansen, J. Vac. Sci. Technol. A **6**, 1778 (1988).
[6]*Properties and Characterization of Amorphous Carbon Films,* edited by J. J. Pouch and S. A. Alterovitz, *Materials Science Forum* Vols. 52 and 53 (Trans. Tech. Publications, Switzerland, 1990).
[7]F. W. Smith, J. Appl. Phys. **55**, 764 (1984).
[8]J. Fink, Th. Muller-Heinzerling, J. Pfluger, B. Scheerer, B. Dichler, P. Koidl, A. Bubenzer, and R. E. Sah, Phys. Rev. B **30**, 4713 (1984).
[9]C. L. Marquardt, R. T. Williams, and D. J. Nagel, in *Plasma Synthesis and Etching of Electronic Materials,* edited by R. P. H. Change and B. Abeles, MRS Symposia Proceedings No. 38 (Materials Research Society, Pittsburgh, 1985), p. 325.
[10]F. Davanloo, E. M. Juengerman, D. R. Jander, T. J. Lee, and C. B. Collins, J. Appl. Phys. **67**, 2081 (1990); C. B. Collins, F. Davanloo, D. R. Jander, T. J. Lee, H. Park, and J. H. You, *ibid.* **69**, 7862 (1991).
[11]J. Krishnaswamy, A. Rengan, J. Narayan, K. Vedam, and C. J. Mchargue, Appl. Phys. Lett. **54**, 2455 (1989).
[12]D. L. Pappas, K. L. Saenger, J. Bruley, W. Krakow, J. J. Cuomo, T. Gu, and R. W. Collins, J. Appl. Phys. **71**, 5675 (1992).
[13]F. Xiong, Y. Y. Wang, V. Leppert, and R. P. H. Chang, J. Mater. Res. (to be published).
[14]S. D. Berger, D. R. McKenzie, and P. J. Martin, Philos. Mag. Lett. **57**, 285 (1988).
[15]R. Lossy, D. L. Pappas, R. A. Roy, J. J. Cuomo, Appl. Phys. Lett. **61**, 171 (1992).
[16]C. Weissmantel, C. Shurer, F. Frohlich, P. Grau, and H. Lehmann, Thin Solid Films **61**, L5 (1979).
[17]J. J. Cuomo, J. P. Doyle, J. Bruley, and J. C. Liu, Appl. Phys. Lett. **58**, 1 (1991); J. Vac. Sci. Technol. A **9**, 2210 (1991).
[18]D. R. McKenzie, D. A. Muller, E. Kravchinskaia, D. Segel, D. J. H. Cockayne, G. Amaratunga, and R. Silva, Thin Solid Films **206**, 198 (1991).
[19]D. R. McKenzie, D. A. Muller, and B. A. Pailthorpe, Phys. Rev. Lett. **67**, 773 (1991).
[20]F. Xiong and R. P. H. Chang, in *Novel Forms of Carbon,* edited by C. L. Renschber, J. Pouch, and D. Cox, MRS Symposia Proceedings No. 270 (Materials Research Society, Pittsburgh, 1985), p. 451.
[21]R. M. A. Azzam and N. M. Bashara, *Ellipsometry and Polarized Light* (North-Holland, Amsterdam, 1989).
[22]H. Raether, in *Excitation of Plasmons and Interband Transitions by Electrons,* edited by G. Hohler, Springer Tracts in Modern Physics, Vol. 88 (Springer-Verlag, Berlin, 1980), p. 1.
[23]J. Daniels, C. V. Festenberg, H. Racther, and K. Zeppenfeld, in *Optical Constants of Solids by Electron Microscopy,* edited by G. Hohler, Springer Tracts in Modern Physics, Vol. 54 (Springer-Verlag, Berlin, 1970), p. 77.
[24]J. Pfluger and J. Fink, *Handbook of Optical Constants of Solids II,* edited by E. D. Palik (Academic, San Diego, 1991), p. 293.
[25]Y. Y. Wang, Ultramicroscopy **33**, 385 (1990).
[26]D. F. Edwards and H. R. Phillipp, in *Handbook of Optical Constants of Solids,* edited by E. D. Palik (Academic, San Diego, 1985), p. 665.
[27]A. Borghesi and G. Guizzetti, in *Handbook of Optical Constants of Solids II* (Ref. 24), p. 449.
[28]D. F. Edwards, in *Handbook of Optical Constants of Solids* (Ref. 26), p. 547.
[29]H. Piller, in *Handbook of Optical Constants of Solids* (Ref. 26), p. 571.
[30]E. A. Taft and H. R. Phillipp, Phys. Rev. **138**, A197 (1965).
[31]T. M. Donovan and W. E. Spicer, J. M. Bennett, and E. J. Ashley, Phys. Rev. B **2**, 397 (1970).
[32]G. A. N. Connell, in *Amorphous Semiconductors,* edited by M. H. Brodsky, Topics in Applied Physics Vol. 36 (Springer, Berlin, 1979), p. 73.
[33]N. Savvides, J. Appl. Phys. **59**, 4133 (1986).
[34]J. D. Joannopoulos and M. Cohen, Phys. Rev. B **35**, 2946 (1987).
[35]J. Robertson and E. P. O'Reilly, Phys. Rev. B **8**, 2733 (1973).
[36]J. Tauc, R. Grigorovici, and A. Vancu, Phys. Status Solidi **15**, 627 (1966).
[37]H. R. Phillipp and H. Ehrenreich, Phys. Rev. **129**, 1550 (1963).
[38]D. Y. Smith, in *Handbook of Optical Constants of Solids* (Ref. 26), p. 35.
[39]N. Savvides, D. R. McKenzie, and R. C. McPhedran, Solid

State Commun. **48**, 189 (1983).
[40]R. Sonenschein, M. Hanfland, and K. Syassen, Phys. Rev. B **38**, 3152 (1988); see Ref. 30 therein.
[41]A. Saeed, P. H. Gaskell, and D. A. Jefferson, Philos. Mag. B **66**, 171 (1992).
[42]P. H. Gaskell, A. Saeed, P. Chieux, and D. R. McKenzie, Philos. Mag. B **66**, 155 (1992).
[43]J. Yuan, A. Saeed, L. M. Brown, and P. H. Gaskell, Philos. Mag. B **66**, 187 (1992).
[44]J. J. Cuomo, D. L. Pappas, J. Bruley, J. P. Doyle, and K. L. Senger, J. Appl. Phys. **10**, 1706 (1991).
[45]F. Xiong and Y. Y. Wang (unpublished).
[46]D. L. Pappas, K. L. Saenger, J. J. Cuomo, and R. W. Dreyfus, J. Appl. Phys. **72**, 3966 (1992).
[47]P. T. Murray, D. T. Peeler, and D. V. Dempsey, in *Phase Formation and Modification by Beam-Solid Interactions,* edited by G. S. Was, L. E. Rehn, and D. Follstaedt, MRS Symposia Proceedings No. 235 (Materials Research Society, Pittsburg, 1992), p. 825.
[48]P. T. Muray (private communication).